

# Stability of the Standard Model vacuum with respect to vacuum tunneling to the Komatsu vacuum in the cMSSM

Hyukjung Kim,<sup>1,\*</sup> Ewan D. Stewart,<sup>2</sup> and Heeseung Zoe<sup>2,†</sup>

<sup>1</sup>*Department of Physics, KAIST, Daejeon 305-701, South Korea*

<sup>2</sup>*Department of Physics, Izmir Institute of Technology,  
Gulbahce, Urla 35430, Izmir, Turkiye*

## Abstract

We investigate the stability of the Standard Model vacuum with respect to vacuum tunneling to the Komatsu vacuum, which exists when  $m_L^2 + m_{H_u}^2 < 0$ , in the cMSSM. Employing the numerical tools **SARAH**, **SPheno** and **CosmoTransitions**, we scan and constrain the parameter space of the cMSSM up to 10 TeV. Regions excluded due to having a vacuum tunneling half-life less than the age of the observable universe are concentrated near the regions where the Standard Model vacuum is tachyonic and are more stringent at smaller  $m_0$ , larger and negative  $A_0$ , and larger  $\tan\beta$ . New excluded regions, which satisfy  $m_h \simeq 125\text{GeV}$ , are found.

---

\* curi951007@gmail.com

† heeseungzoe@iyte.edu.tr

## I. INTRODUCTION

The Minimal Supersymmetric Standard Model (MSSM) [1–3] is one of the most compelling models for physics beyond the Standard Model, as its minimal combination of the Standard Model and supersymmetry not only provides a solution to the hierarchy problem but also predictions that have been confirmed by experiments. First, assuming gauge coupling unification and a supersymmetry mass scale in the range of  $10^2$  to  $10^4$  GeV, the MSSM correctly [4, 5] predicted [6, 7] a relation between the Standard Model gauge couplings. Second, the MSSM has consistently predicted the Higgs mass  $m_h \lesssim 130$  GeV since well before the LHC [8–10]. Combined with the experimental bound of  $m_h \gtrsim 114$  GeV from the Large Electron–Positron Collider (LEP) [11], the MSSM thus predicted the Higgs boson mass within a 10% range of the value observed at the LHC [12, 13].

In the MSSM, the superpartners of the Standard Model particles were expected to be found in the range of  $10^2$  to  $10^4$  GeV and have been searched for in experiments such as the Large Hadron Collider (LHC). The observation of the Higgs boson mass at 125 GeV and recent searches have constrained the stop and gluino masses to be above 1 TeV [14–19]. More generally, the LHC has increased the lower bound of the supersymmetric particle masses [18–23], and the difference between the electroweak scale and the supersymmetric particle mass scale has become a fine-tuning problem known as the little hierarchy problem.

The Muon g-2 experiment conducted by Brookhaven National Laboratory [24] and Fermilab [25, 26] has measured the anomalous magnetic moment of the muon to 20 significant figures. Theoretical estimates of muon g-2 in the Standard Model derived using electron collision data [27] show a  $5\sigma$  significance difference with the experiment, but lattice QCD simulation of the Standard Model [28] agrees with the experimental results. Which calculation is correct will determine whether the g-2 experiment is evidence of physics beyond the Standard Model.

Despite a large region of parameter space being ruled out by experiments, the MSSM is still a compelling candidate for physics beyond the Standard Model, especially compared to its alternatives, such as extra dimensions [29, 30], composite Higgs [31–33] and cosmological relaxation [34], which lack successful predictions. It is expected to see clear evidence for the MSSM in a future collider that can detect sparticles with masses up to 10 TeV [35–37].

The MSSM has a high dimensional scalar field space, whose potential may have multiple

vacua [38–42], which should satisfy the cosmological requirement that the tunneling half-life from the Standard Model vacuum to the other vacua should not be much less than the age of the observable universe.

Calculating tunneling in one-dimensional field space is straightforward, but finding the instanton path in multi-dimensional field space is difficult. However, various numerical packages have been developed over the last decade [43–45] and used to constrain MSSM parameters [46–53]. In Ref. [46], the authors scan and constrain the cMSSM parameters up to 4 TeV for vacuum tunneling to vacua formed by  $h_u, h_d, u_3, \bar{u}_3, e_3, \bar{e}_3$ . In Ref. [47], the parameter space of the Natural MSSM is constrained using vacuum and thermal tunneling with non-zero  $h_u, h_d, u_3, \bar{u}_3$ . No points satisfying the Higgs mass constraint  $m_h \simeq 125$  GeV were excluded by vacuum tunneling, but some were by thermal tunneling. In Ref. [48], the authors assume neutralino dark matter with stau-coannihilation and the theoretical estimate of muon g-2 and find points which best fit with dark matter abundance, muon g-2, and the Higgs mass and decay rate. These points are tested by vacuum tunneling to the Komatsu vacuum and they are found to be safe. Several other papers [49–53] use vacuum tunneling to further reduce the parameter space that survives after making various assumptions and applying constraints. In this paper, we scan and constrain the full cMSSM parameter space up to 10 TeV by vacuum tunneling to the Komatsu vacuum.

The Komatsu vacuum [40, 54] lies in the direction

$$\mu H_u L_k = \lambda_d^{ij} \bar{d}_i Q_j L_k + \lambda_e^{ij} \bar{e}_i L_j L_k \quad (1)$$

along which the  $\mu$  term contribution to  $LH_u$ 's mass squared is cancelled. At large values of  $LH_u$ , the D-term constrains  $|L| \simeq |H_u|$  and if

$$m_L^2 + m_{H_u}^2 < 0 \quad (2)$$

the potential descends into a deep vacuum, where it is stabilized by higher-order terms such as supersymmetric neutrino mass terms.

In Section II, we present the potential used in this paper and briefly review the calculation of vacuum tunneling. In Section III, we illustrate the tunneling calculation process, including a brief explanation of the numerical tools: SARAH [55], SPheno [56] and CosmoTransitions [43]. In Section IV, we plot the region excluded by vacuum tunneling to the Komatsu vacuum in cMSSM parameter space. We summarize the results and suggest future work in Section V.

## II. MODEL

The MSSM superpotential is

$$W = \lambda_u^{ij} \bar{u}_i Q_j H_u - \lambda_d^{ij} \bar{d}_i Q_j H_d - \lambda_e^{ij} \bar{e}_i L_j H_d + \mu H_u H_d \quad (3)$$

There are two types of Komatsu vacuum: quark Komatsu vacuum  $\mu H_u L_k = \lambda_d^{ij} \bar{d}_i Q_j L_k$  and lepton Komatsu vacuum  $\mu H_u L_k = \lambda_e^{ij} \bar{e}_i L_j L_k$ . We have sampled the tunneling rate for the quark Komatsu vacuum and found it to be consistently less than that for the lepton Komatsu vacuum. Thus, we restrict to the lepton Komatsu vacuum

$$\mu H_u L_k = \lambda_e^{ij} \bar{e}_i L_j L_k \quad (4)$$

Note that  $L_j L_k = 0$  if  $j = k$ , so we need to consider at least two lepton generations. We neglect the off-diagonal Yukawa couplings and reduce the field space by the following three criteria. First, we build the potential relevant to the Standard Model and lepton Komatsu vacua by using  $H_u, H_d, L$  and  $\bar{e}$ , and setting  $Q = \bar{u} = \bar{d} = 0$ . Second, we choose the combination of lepton generations which gives the largest tunneling rate. When the Yukawa coupling  $\lambda_e^{ij}$  is large,  $\bar{e}_i L_j$  can be small but still cancel the  $\mu$  contribution to  $LH_u$ 's mass squared, resulting in a saddle point close to the origin and a large tunneling rate. Hence, we use  $\lambda_e^{33} \bar{e}_3 L_3$  and set  $\bar{e}_1 = \bar{e}_2 = 0$ . On the other hand, a larger Yukawa coupling renormalises the corresponding slepton mass squared to smaller values at low energy, increasing the tunneling rate. Hence we set  $L_1 = 0$  and use  $L_2$ . Third, we use  $SU(2)$  gauge freedom to set  $h_u^+ = 0$ . Then  $e_2 = \nu_3 = h_d^- = 0$  follows because the fields have no destabilizing linear terms. Thus, the field configuration we use in this paper is

$$H_u = \begin{pmatrix} 0 \\ h_u \end{pmatrix}, H_d = \begin{pmatrix} h_d \\ 0 \end{pmatrix}, L_2 = \begin{pmatrix} \nu_2 \\ 0 \end{pmatrix}, L_3 = \begin{pmatrix} 0 \\ e_3 \end{pmatrix}, \bar{e}_3 = \bar{e}_3 \quad (5)$$

and other fields zero.

At tree-level our potential is

$$\begin{aligned} V_{\text{tree}} = & m_{H_u}^2 |h_u|^2 + m_{H_d}^2 |h_d|^2 + m_{L_2}^2 |\nu_2|^2 + m_{L_3}^2 |e_3|^2 + m_{\bar{e}_3}^2 |\bar{e}_3|^2 \\ & + [(a_e^{33} \bar{e}_3 e_3 h_d - B \mu h_u h_d) + \text{c.c.}] + |\lambda_e^{33} \bar{e}_3 h_d|^2 + |\mu h_u - \lambda_e^{33} \bar{e}_3 e_3|^2 \\ & + \frac{1}{8} g_1^2 (|h_u|^2 - |h_d|^2 - |\nu_2|^2 - |e_3|^2 + 2|\bar{e}_3|^2)^2 + \frac{1}{8} g_2^2 (|h_u|^2 - |h_d|^2 - |\nu_2|^2 + |e_3|^2)^2 \end{aligned} \quad (6)$$

The tunneling rate to the Komatsu vacuum is calculated by the well-known instanton method [57], which gives a tunneling rate

$$\Gamma = Ae^{-S_E} \quad (7)$$

where the prefactor  $A$  comes from the measure of the path integral and includes fluctuations around the instanton, and  $S_E$  is the Euclidean action given by

$$S_E = 2\pi^2 \int_0^\infty \rho^3 d\rho \left[ \frac{1}{2} h_{ab} \frac{\partial \phi^a}{d\rho} \frac{\partial \phi^b}{d\rho} + V(\phi) \right] \quad (8)$$

where  $\rho$  is the radial distance in Euclidean space. The field space vector

$$\phi = (h_u, h_d, \nu_2, e_3, \bar{e}_3) \quad (9)$$

and  $h_{ab}$  is the metric on field space. The equation of motion for the instanton tunneling from false vacuum  $\phi_f$  to true vacuum  $\phi_t$  is

$$\frac{d^2 \phi^a}{d\rho^2} + \frac{3}{\rho} \frac{d\phi^a}{d\rho} = h^{ab} \frac{\partial V}{\partial \phi^b} \quad (10)$$

with the boundary conditions  $\frac{d\phi}{d\rho}(0) = 0$ ,  $\phi(0) = \phi_t$  and  $\phi(\infty) = \phi_f$ .

### III. METHOD

#### A. Numerical tools

We use **SARAH** [55] to generate the one-loop corrected potential and source file for **SPheno** [56]. We calculate the supersymmetric particle spectrum with **SPheno**, including masses and Yukawa couplings at a two-loop level. We use **CosmoTransitions** [43] to calculate the multi-field tunneling. It decomposes the instanton equation into parallel and perpendicular to the path and searches for the instanton path, which is the solution for both parallel and perpendicular equations.

#### B. Tunneling to Komatsu vacuum

The calculation process is illustrated in Figure 1. We work in the context of the cMSSM [58], which simplifies MSSM parameters into five parameters: the universal scalar mass  $m_0$ ,

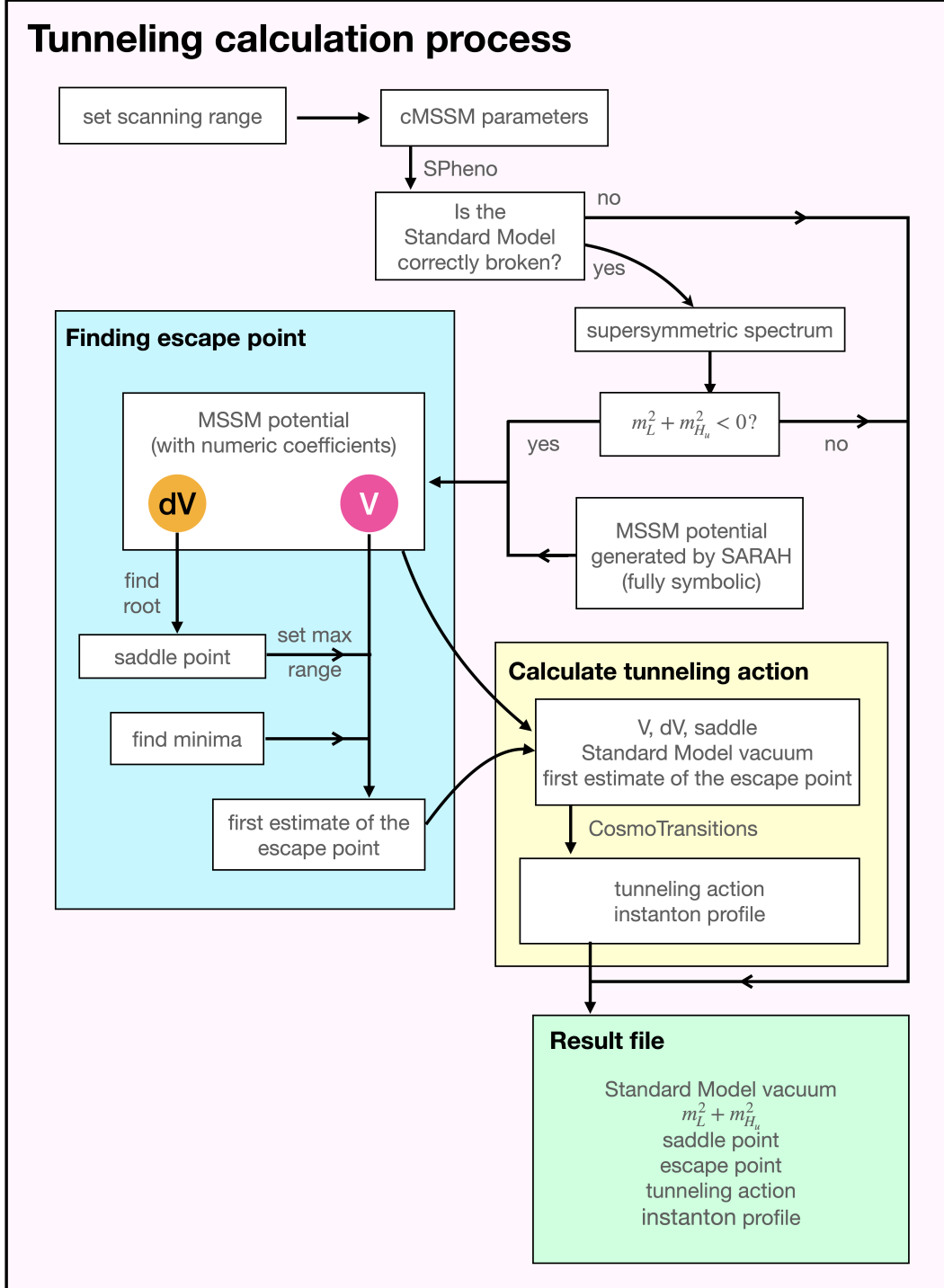


FIG. 1. Full process of tunneling calculation

the ratio between the MSSM Higgs vacuum expectation values  $\tan \beta$ , the universal gaugino mass  $m_{1/2}$ , and the universal trilinear coupling  $A_0$ , as well as the sign of  $\mu$ . The scanning range for the cMSSM parameters is shown in TABLE I.

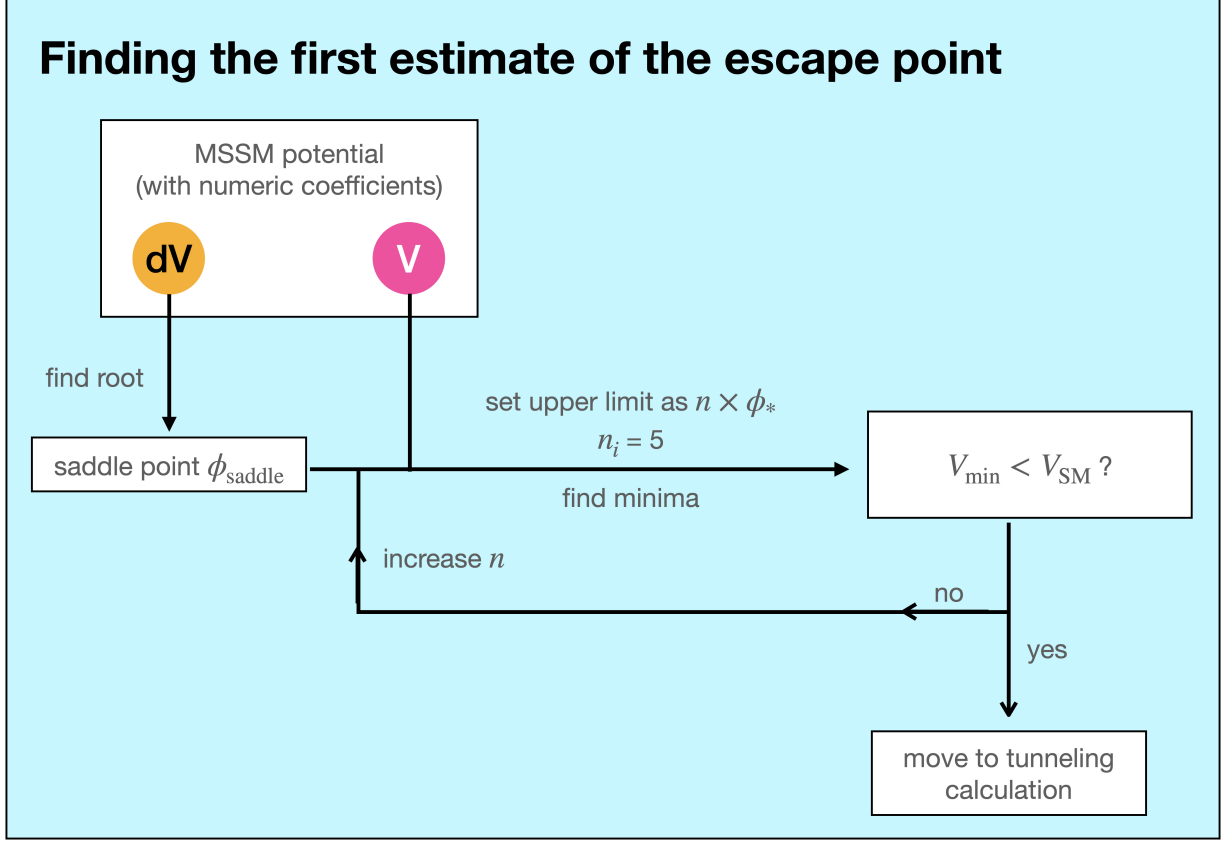


FIG. 2. Detailed process of searching for the first estimate of the escape point

Parameter	Range
$m_0/\text{TeV}$	$\{0.1, 0.2, 0.5, 1, 2, 5, 10\}$
$\tan \beta$	$\{10, 20, 30, 40, 50\}$
$\log_{10}(m_{1/2}/\text{TeV})$	$[-1, 1]$
$\log_{10}( A_0 /\text{TeV})$	$[-1, 1]$
sign of $\mu$	+

TABLE I. Scanning range in cMSSM parameter space

We start by setting the scanning range of the cMSSM parameters. **SPheno** checks whether the Standard Model vacuum is correctly broken and generates a SUSY spectrum. Next, the existence of the Komatsu vacuum is checked by the sign of  $m_L^2 + m_{H_u}^2$ . If the Komatsu vacuum exists, we move to find the first estimate of the escape point.

We look for the escape point of the bounce solution for potentials unbounded from below in the following manner. First, we find the saddle point and set  $\phi_* = 5 \times \max \{h_u, h_d, \nu_2, e_3, \bar{e}_3\}_{\text{saddle}}$

to choose the initial scanning range for finding the escape point. We find the minimum of the potential within the range  $\phi^a < \phi_*$  for each  $a$  by using the `minimize` function in `Scipy`. If the Standard Model vacuum is found as the minimum, we continuously extend the scanning range to  $\phi^a < n\phi_*$  for some positive integer  $n$  until we find a proper minimum, which we take as a first estimate of the escape point. The process of finding the first estimate of the escape point is shown in Figure 2. Finally, we calculate the bounce action with `CosmoTransitions` and save the results, including the location of the Standard Model vacuum, the escape point and the value of the tunneling action.

#### IV. RESULTS

The constraints on the cMSSM parameter space derived by considering vacuum tunneling from the Standard Model vacuum to the lepton Komatsu vacuum are plotted in Figure 3. We set the prefactor  $A$  in Eq. (7) to  $\text{TeV}^4$ , and the action threshold for determining dangerous tunneling to 410, which corresponds to a tunneling half-life of the order of the age of the observable universe. We set the spread of the Higgs mass constraint as 1 GeV, which is the theoretical uncertainty of the Higgs mass calculation in `SPheno` [59, 60].

There are four notable trends in the tunneling constraints. First, regions excluded by tunneling (yellow) are located near the regions where the Standard Model is tachyonic (red). The sparticles are close to tachyonic near the red regions, so the height of the saddle is lower, reducing the action. Second, the constraints are stronger for smaller  $m_0$  because the mass squareds are smaller, lowering the height of the saddle. Third, the constraints are stronger for larger  $\tan\beta$  since  $\lambda_e$  is larger allowing  $\bar{e}_i L_j$  to be smaller, but still cancel the  $\mu$  contribution to mass squared of  $LH_u$ , resulting in a saddle point located nearer the origin and a smaller action. Fourth, the constraints are stronger for large and negative  $A_0$ . For negative  $A_0$ , the trilinear couplings are larger in magnitude at low energy, which renormalises the mass squareds to be smaller at low energy, lowering the height of the saddle.

Our main findings are as follows. For  $\tan\beta \leq 30$ , only a few points near the tachyonic region are excluded by tunneling and they don't satisfy the Higgs mass constraint. However, for  $\tan\beta = 40, 50$ , we find a region, enlarged in Figure 4, satisfying the Higgs mass constraint but excluded by tunneling, which has not been reported previously.

We have also scanned using the one-loop corrected potential but the tunneling results are



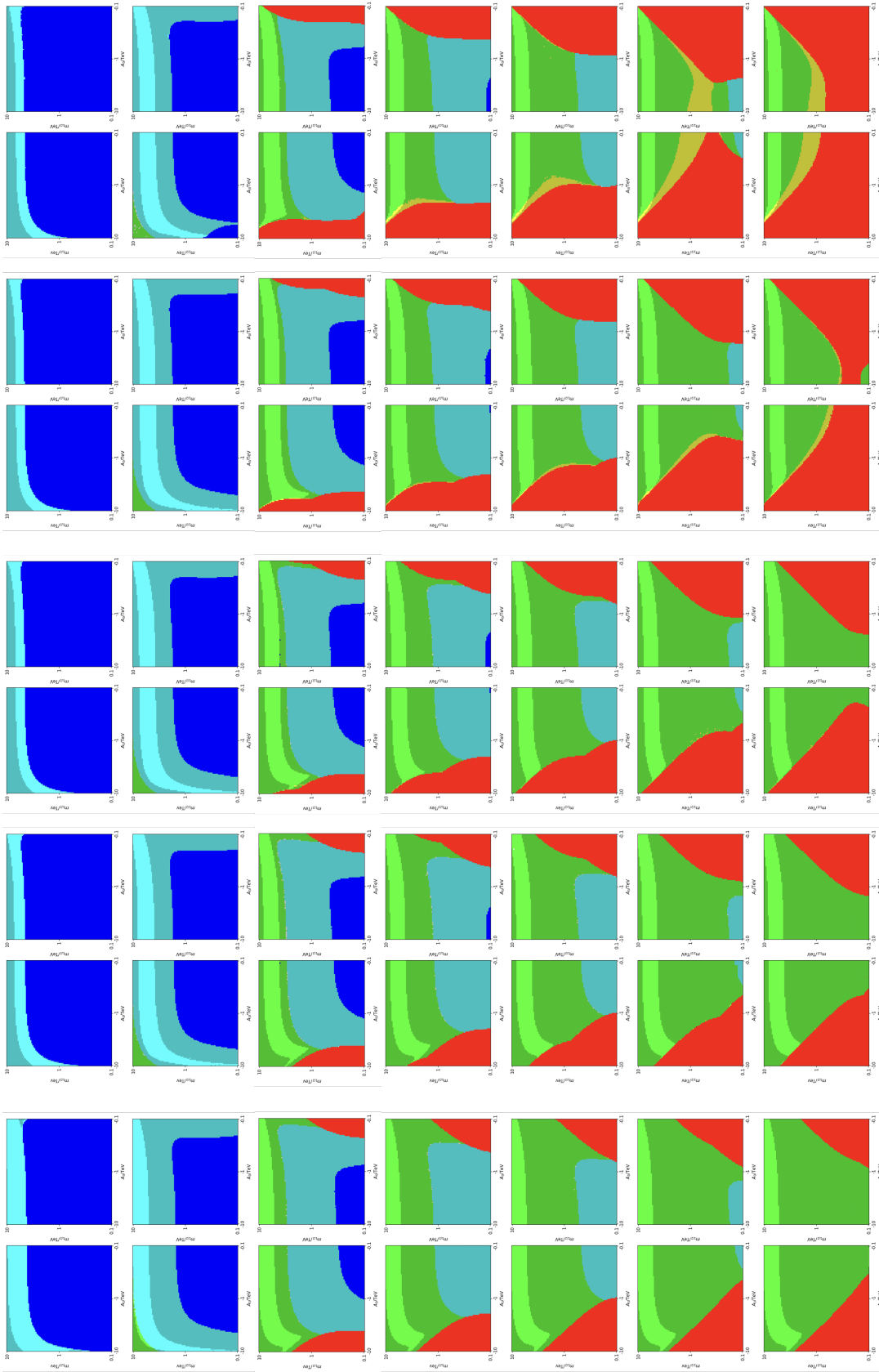


FIG. 3. Constraints from vacuum tunneling to the lepton Komatsu vacuum in cMSSM parameter space. Left to right:  $\tan\beta = 10, 20, 30, 40, 50$ ; bottom to top:  $m_0 = 0.1, 0.2, 0.5, 1, 2, 5, 10 \text{ TeV}$ . ■ tachyonic Standard Model vacuum; ■, ■, ■, ■  $S < 410$ ; ■, ■, ■  $S > 410$ ; ■, ■, ■, ■, ■  $m_h \neq 125.25 \pm 1 \text{ GeV}$ ; ■, ■, ■, ■, ■  $m_h = 125.25 \pm 1 \text{ GeV}$ ; ■, ■, ■, ■, ■ no electroweak symmetry breaking; ■, ■, ■, ■, ■ no Komatsu vacuum; ■, ■, ■, ■, ■  $m_h \neq 125.25 \pm 1 \text{ GeV}$ .

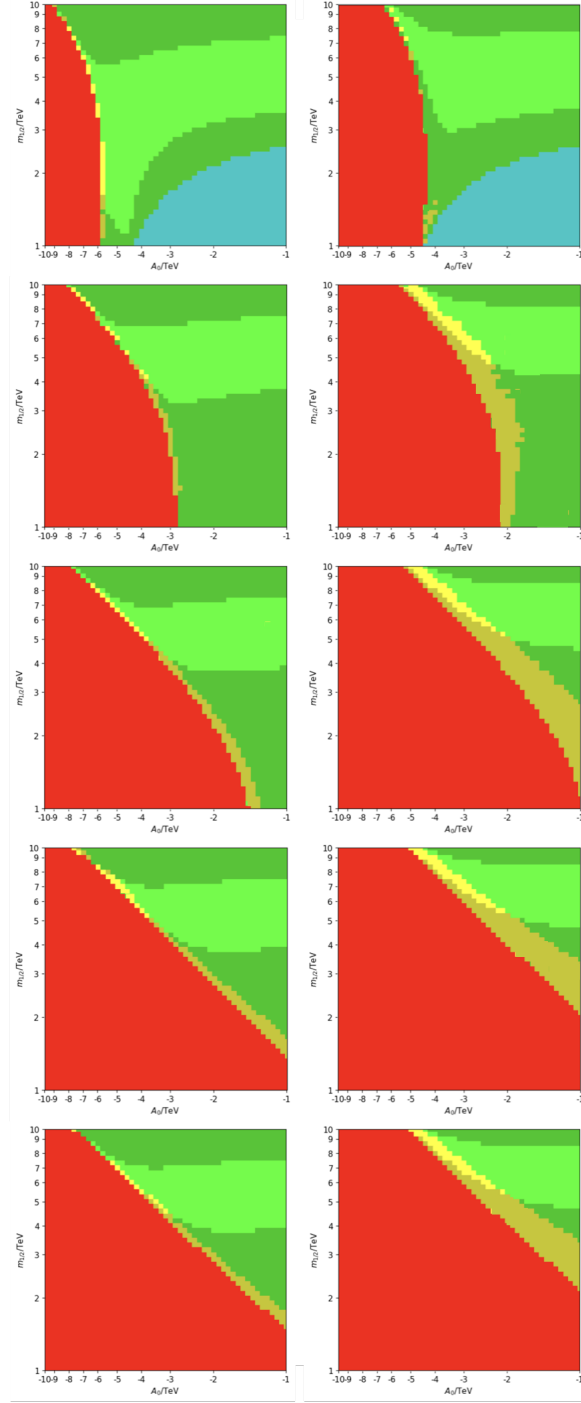


FIG. 4. Enlargement of the region satisfying the Higgs mass constraint but excluded by tunneling. Left to right:  $\tan \beta = 40, 50$ ; Bottom to top:  $m_0 = 0.1, 0.2, 0.5, 1, 2$  TeV. Color representation is the same as in Figure 3.

not significantly different compared to those of tree-level potential tunneling. We did not consider the full one-loop corrections to the tunneling [61].

## V. SUMMARY

In this paper, we have constrained the cMSSM parameter space up to 10 TeV by requiring the vacuum tunneling half-life to the lepton Komatsu vacuum to be greater than the age of the observable universe. The results in Figure 3 show that the tunneling constraints are significant only at  $\tan\beta = 40, 50$  and  $m_0 < 2$  TeV, and the excluded regions are situated near where the Standard Model is tachyonic. Figure 4 enlarges the region satisfying the Higgs mass constraint but excluded by tunneling. The constraints from vacuum tunneling are not strong, but they are model-independent and robust. We expect to see stronger constraints from thermal tunneling, but they will be less robust as they will depend on the cosmological history.

## ACKNOWLEDGEMENTS

This work is supported by TÜBİTAK-ARDEB-1001 program under project 123F257.

- 
- [1] S. P. Martin, Adv. Ser. Direct. High Energy Phys. **18**, 1 (1998), arXiv:hep-ph/9709356.
  - [2] I. J. R. Aitchison, *Supersymmetry and the MSSM: An Elementary introduction* (2005) arXiv:hep-ph/0505105.
  - [3] C. Csaki, Mod. Phys. Lett. A **11**, 599 (1996), arXiv:hep-ph/9606414.
  - [4] U. Amaldi, W. de Boer, and H. Furstenau, Phys. Lett. B **260**, 447 (1991).
  - [5] W. Martens, L. Mihaila, J. Salomon, and M. Steinhauser, Phys. Rev. D **82**, 095013 (2010), arXiv:1008.3070 [hep-ph].
  - [6] M. B. Einhorn and D. R. T. Jones, Nucl. Phys. B **196**, 475 (1982).
  - [7] S. Dimopoulos and H. Georgi, Nucl. Phys. B **193**, 150 (1981).
  - [8] R. Hempfling and A. H. Hoang, Phys. Lett. B **331**, 99 (1994), arXiv:hep-ph/9401219.
  - [9] G. Degrandi, P. Slavich, and F. Zwirner, Nucl. Phys. B **611**, 403 (2001), arXiv:hep-ph/0105096.

- [10] A. Brignole, G. Degrossi, P. Slavich, and F. Zwirner, Nucl. Phys. B **643**, 79 (2002), arXiv:hep-ph/0206101.
- [11] R. Barate *et al.* (LEP Working Group for Higgs boson searches, ALEPH, DELPHI, L3, OPAL), Phys. Lett. B **565**, 61 (2003), arXiv:hep-ex/0306033.
- [12] S. Chatrchyan *et al.* (CMS), Phys. Lett. B **716**, 30 (2012), arXiv:1207.7235 [hep-ex].
- [13] R. L. Workman *et al.* (Particle Data Group), PTEP **2022**, 083C01 (2022).
- [14] P. Draper, P. Meade, M. Reece, and D. Shih, Phys. Rev. D **85**, 095007 (2012), arXiv:1112.3068 [hep-ph].
- [15] S. Heinemeyer, O. Stal, and G. Weiglein, Phys. Lett. B **710**, 201 (2012), arXiv:1112.3026 [hep-ph].
- [16] F. Brummer, S. Kraml, and S. Kulkarni, JHEP **08**, 089 (2012), arXiv:1204.5977 [hep-ph].
- [17] P. Slavich *et al.*, Eur. Phys. J. C **81**, 450 (2021), arXiv:2012.15629 [hep-ph].
- [18] M. Aaboud *et al.* (ATLAS), Phys. Rev. D **98**, 032008 (2018), arXiv:1803.10178 [hep-ex].
- [19] A. M. Sirunyan *et al.* (CMS), Eur. Phys. J. C **79**, 444 (2019), arXiv:1901.06726 [hep-ex].
- [20] C. Han, K.-i. Hikasa, L. Wu, J. M. Yang, and Y. Zhang, Phys. Lett. B **769**, 470 (2017), arXiv:1612.02296 [hep-ph].
- [21] W. Adam and I. Vivarelli, Int. J. Mod. Phys. A **37**, 2130022 (2022), arXiv:2111.10180 [hep-ex].
- [22] G. Aad *et al.* (ATLAS), Phys. Rev. D **90**, 052008 (2014), arXiv:1407.0608 [hep-ex].
- [23] V. Khachatryan *et al.* (CMS), Eur. Phys. J. C **76**, 460 (2016), arXiv:1603.00765 [hep-ex].
- [24] G. W. Bennett *et al.* (Muon g-2), Phys. Rev. D **73**, 072003 (2006), arXiv:hep-ex/0602035.
- [25] B. Abi *et al.* (Muon g-2), Phys. Rev. Lett. **126**, 141801 (2021), arXiv:2104.03281 [hep-ex].
- [26] D. P. Aguillard *et al.* (Muon g-2), (2023), arXiv:2308.06230 [hep-ex].
- [27] T. Aoyama *et al.*, Phys. Rept. **887**, 1 (2020), arXiv:2006.04822 [hep-ph].
- [28] S. Borsanyi *et al.*, Nature **593**, 51 (2021), arXiv:2002.12347 [hep-lat].
- [29] N. Arkani-Hamed, S. Dimopoulos, and G. R. Dvali, Phys. Lett. B **429**, 263 (1998), arXiv:hep-ph/9803315.
- [30] L. Randall and R. Sundrum, Phys. Rev. Lett. **83**, 3370 (1999), arXiv:hep-ph/9905221.
- [31] V. A. Miransky, M. Tanabashi, and K. Yamawaki, Phys. Lett. B **221**, 177 (1989).
- [32] R. S. Chivukula, B. A. Dobrescu, H. Georgi, and C. T. Hill, Phys. Rev. D **59**, 075003 (1999), arXiv:hep-ph/9809470.

- [33] C. T. Hill and E. H. Simmons, Phys. Rept. **381**, 235 (2003), [Erratum: Phys.Rept. 390, 553–554 (2004)], arXiv:hep-ph/0203079.
- [34] P. W. Graham, D. E. Kaplan, and S. Rajendran, Phys. Rev. Lett. **115**, 221801 (2015), arXiv:1504.07551 [hep-ph].
- [35] A. Abada *et al.* (FCC), Eur. Phys. J. C **79**, 474 (2019).
- [36] A. Abada *et al.* (FCC), Eur. Phys. J. ST **228**, 261 (2019).
- [37] A. Abada *et al.* (FCC), Eur. Phys. J. ST **228**, 755 (2019).
- [38] M. Drees, M. Gluck, and K. Grassie, Phys. Lett. B **157**, 164 (1985).
- [39] A. Kusenko, P. Langacker, and G. Segre, Phys. Rev. D **54**, 5824 (1996), arXiv:hep-ph/9602414.
- [40] H. Komatsu, Phys. Lett. B **215**, 323 (1988).
- [41] J. A. Casas, A. Lleyda, and C. Munoz, Nucl. Phys. B **471**, 3 (1996), arXiv:hep-ph/9507294.
- [42] A. Strumia, Nucl. Phys. B **482**, 24 (1996), arXiv:hep-ph/9604417.
- [43] C. L. Wainwright, Comput. Phys. Commun. **183**, 2006 (2012), arXiv:1109.4189 [hep-ph].
- [44] R. Sato, Comput. Phys. Commun. **258**, 107566 (2021), arXiv:1908.10868 [hep-ph].
- [45] V. Guada, M. Nemevšek, and M. Pintar, Comput. Phys. Commun. **256**, 107480 (2020), arXiv:2002.00881 [hep-ph].
- [46] J. E. Camargo-Molina, B. O’Leary, W. Porod, and F. Staub, JHEP **12**, 103 (2013), arXiv:1309.7212 [hep-ph].
- [47] J. E. Camargo-Molina, B. Garbrecht, B. O’Leary, W. Porod, and F. Staub, Phys. Lett. B **737**, 156 (2014), arXiv:1405.7376 [hep-ph].
- [48] P. Bechtle *et al.*, Eur. Phys. J. C **76**, 96 (2016), arXiv:1508.05951 [hep-ph].
- [49] U. Chattopadhyay and A. Dey, Journal of High Energy Physics **2014** (2014), 10.1007/jhep11(2014)161.
- [50] W. G. Hollik, Journal of High Energy Physics **2016** (2016), 10.1007/jhep08(2016)126.
- [51] G. H. Duan, C. Han, B. Peng, L. Wu, and J. M. Yang, Phys. Lett. B **788**, 475 (2019), arXiv:1809.10061 [hep-ph].
- [52] W. G. Hollik, G. Weiglein, and J. Wittbrodt, JHEP **03**, 109 (2019), arXiv:1812.04644 [hep-ph].
- [53] W. G. Hollik, S. Liebler, G. Moortgat-Pick, S. Paßehr, and G. Weiglein, The European Physical Journal C **79** (2019), 10.1140/epjc/s10052-019-6561-6.

- [54] S. A. Abel and C. A. Savoy, Nucl. Phys. B **532**, 3 (1998), arXiv:hep-ph/9803218.
- [55] F. Staub, Comput. Phys. Commun. **185**, 1773 (2014), arXiv:1309.7223 [hep-ph].
- [56] W. Porod and F. Staub, Comput. Phys. Commun. **183**, 2458 (2012), arXiv:1104.1573 [hep-ph].
- [57] S. R. Coleman, Phys. Rev. D **15**, 2929 (1977), [Erratum: Phys.Rev.D 16, 1248 (1977)].
- [58] G. L. Kane, C. F. Kolda, L. Roszkowski, and J. D. Wells, Phys. Rev. D **49**, 6173 (1994), arXiv:hep-ph/9312272.
- [59] H. Bahl, S. Heinemeyer, W. Hollik, and G. Weiglein, The European Physical Journal C **80** (2020), 10.1140/epjc/s10052-020-8079-3.
- [60] F. Staub and W. Porod, The European Physical Journal C **77** (2017), 10.1140/epjc/s10052-017-4893-7.
- [61] V. Guada and M. Nemevšek, Phys. Rev. D **102**, 125017 (2020), arXiv:2009.01535 [hep-th].